Linkage of Monovalent and Divalent Ion Binding in the Folding of the P4−P6 Domain of the Tetrahymena Ribozyme †

ARTICLE *in* BIOCHEMISTRY · MAY 2002

Impact Factor: 3.02 · DOI: 10.1021/bi020042v · Source: PubMed

5 AUTHORS, INCLUDING:

Takeshi Uchida
Hokkaido University
51 PUBLICATIONS **1,077** CITATIONS
SEE PROFILE

Corie Ralston
University of California, Berkeley
42 PUBLICATIONS **936** CITATIONS
SEE PROFILE

Linkage of Monovalent and Divalent Ion Binding in the Folding of the P4−P6 Domain of the *Tetrahymena* Ribozyme†

Takeshi Uchida,‡,§ Qin He,‡,§ Corie Y. Ralston,‡,§ Michael Brenowitz,‡,|| and Mark R. Chance*,‡,§,||

Center for Synchrotron Biosciences, Department of Physiology and Biophysics, and Department of Biochemistry, Albert Einstein College of Medicine of Yeshiva University, 1300 Morris Park Avenue, Bronx, New York 10461

Received January 16, 2002; Revised Manuscript Received March 12, 2002

ABSTRACT: We have explored the linkage of monovalent and divalent ion binding in the folding of the P4−P6 domain of *Tetrahymena thermophila* ribozyme by examining the Mg^{2+}-induced folding and the urea-induced denaturation of the folded state as a function of Na^+ under equilibrium folding conditions using hydroxyl radical footprinting. These studies allowed a thermodynamic examination of eight discrete protection sites within P4−P6 that are involved in several tertiary structure contacts. Monovalent ions compete with Mg^{2+} ions in mediating P4−P6 folding. The urea denaturation isotherms demonstrated $\Delta\Delta G$ values of >2 kcal mol^{-1} in experiments conducted in 10 versus 200 mM NaCl at a constant 10 mM $MgCl_2$. However, the individual-site isotherms reported by footprinting revealed that larger than average changes in ΔG values were localized to specific sites within the Mg^{2+}-rich A-bulge. The competitive effects of monovalent ions were less when K^+ rather than Na^+ was the monovalent cation present. This result indicates the importance of the specific K^+ binding sites that are associated with AA-platform structures to P4−P6 folding and stability. These site-specific footprinting data provide quantitative and site-specific measurements of the ion-linked stability for P4−P6 that are interpreted with respect to crystallographic data.

To achieve compact folded structures in the face of the electrostatic repulsion of its phosphate backbone, RNA molecules bind monovalent and divalent cations to neutralize the anionic phosphates of the backbone. The important role of Mg^{2+} in stabilizing RNA tertiary structure is well-known. In early studies of tRNA folding, Mg^{2+} ions were found to stabilize the tertiary structure of the RNA and reconstitute its biological activity (*1*). Moreover, many studies have shown that Mg^{2+} is also important in assembling specific tertiary structures and recovering functions of other RNAs as well as tRNA. For example, the *Tetrahymena* group I intron requires millimolar concentrations of Mg^{2+} to fold into a functionally active structure (*2*), and a pseudoknot derived from the *Escherichia coli* α-mRNA is effectively stabilized by Mg^{2+} (*3*). Direct visualization of Mg^{2+} ions in high-resolution X-ray crystal structures of yeast $tRNA^{Phe}$ and the *Tetrahymena* ribozyme have allowed an understanding of the specific coordination of divalent ions and their role in stabilizing tertiary structure (*4*−*6*).

Monovalent ions as well as Mg^{2+} are involved in electrostatic interactions stabilizing tertiary structure of RNA. Specifically bound NH_4^+ stabilizes the tertiary structure of a conserved domain of the large-subunit ribosomal RNA (*7*). The hammerhead, hairpin, and VS ribozymes are all active at high concentrations of monovalent ion without the presence of divalent ions (*8*). Basu et al. (*9*) has also identified site-specific coordination of K^+ ion in the P4−P6 subdomain of the *Tetrahymena* ribozyme. Recent studies point to a role for condensed counterions in mediating the electrostatic collapse of RNA during folding (*10*−*12*). Together, these studies highlight the important role for monovalent ions in stabilizing the highly compacted structure characteristic of many RNAs.

The folding of the *Tetrahymena* L-21 ribozyme has been extensively studied using a variety of techniques, including activity assays, chemical modification by Fe(II)-EDTA-based hydroxyl radical, synchrotron X-ray footprinting, X-ray scattering, and RNase cleavage (*13*−*23*). Also, a number of studies have examined stable subdomains of the ribozyme that can fold independently. For example, the 160-nt P4−P6 domain, as well as its P5abc substructure, can fold independently, and hydroxyl radical footprinting reveals internal tertiary contacts similar to those seen in the native ribozyme (*24*). Equilibrium folding studies as a function of Mg^{2+} concentration for both P4−P6 and the L-21 ribozyme (*13*, *24*) have determined that small differences in thermodynamic parameters (e.g., apparent binding constants and Hill coefficients) exist for the formation of different tertiary contacts as monitored by footprinting. Typically, at low monovalent ion concentration (typically 30 mM or less) the midpoints for the formation of tertiary contacts within the independently folding domains P5abc and P4−P6 are slightly lower than those for the catalytic core within the full-length ribozyme.

† This research is supported by grants from the Biomedical Technology Program of the National Center for Research Resources, NIH-RR-01633, and the National Institute for General Medical Sciences, NIH-GM-52348.

* Corresponding author. Telephone: 718-430-4136. Fax: 718-430-8587. E-mail: mrc@aecom.yu.edu.

‡ Center for Synchrotron Biosciences.

§ Department of Physiology and Biophysics.

|| Department of Biochemistry.

10.1021/bi020042v CCC: $22.00
Published on Web 04/16/2002

When folding is examined in real time after the addition of Mg^{2+} by using synchrotron-based hydroxyl radical footprinting, the process is initiated by concerted formation of numerous tertiary contacts within the P4−P6 structure at a rate of ~1−2 s^{-1} at low monovalent ion concentrations (*14*). The peripheral domains fold subsequently with rates of 0.3 s^{-1}, while protections within the catalytic core appear much more slowly. The folding of isolated P4−P6 domain is also concerted with rates similar to those observed for the full-length ribozyme at low monovalent ion concentrations. Significant acceleration of the folding rate to >30 s^{-1} was seen as the concentration of monovalent cation was increased (*16*, *25*). Studies of the global conformation of RNAs have shown that monovalent ions compact both P4−P6 and the L-21 RNA in the absence of Mg^{2+}, perhaps reducing the entropic barrier to folding (*11*, *16*, *22*). It is necessary to understand the effects of monovalent ions on RNA structure in order to interpret these effects on the folding mechanism.

By combining urea denaturation and footprinting, the stability as well as the cooperative coupling of individual tertiary contacts of RNA can be individually monitored (*15*). In this investigation, Mg^{2+}-folding and urea-unfolding hydroxyl radical footprinting equilibrium experiments were carried out as a function of monovalent ion concentration in order to probe site-specific effects on stability. We determined thermodynamic parameters for eight hydroxyl radical protections in the P4−P6 domain, corresponding to several discrete tertiary contacts. The results suggest that monovalent ion competes with site-specifically bound Mg^{2+} ions in the A-rich bulge of P4−P6 (*6*, *26*) and that this competition destabilizes P4−P6 ~15-fold for 200 versus 10 mM NaCl. In addition, a small stabilizing effect of the K^+ ion compared to Na^+ is observed, which may be related to K^+ binding in AA-platform sites identified in the crystal structure of P4−P6 (*9*).

EXPERIMENTAL PROCEDURES

RNA Preparation. P4−P6 RNA was prepared by in vitro transcription and purified as previously described (*27*). RNA was labeled at the 5′ end with [γ-^{32}P]ATP using T4 polynucleotide kinase and repurified by 4% polyacrylamide/7 M urea gels.

Mg^{2+}-Folding Isotherms. The sites of the RNA protected against hydroxyl radical attack were determined using Fe(II)-EDTA footprinting (*2*, *28*) as described previously (*13*, *15*). In the Mg^{2+}-induced folding experiment, the 5′-^{32}P-labeled P4−P6 samples were denatured by heating to 95 °C for 1 min in CE buffer (10 mM sodium cacodylate and 0.1 mM EDTA) to which was added the indicated concentration of monovalent ion. After the addition of various concentrations of Mg^{2+}, the solution was equilibrated at 42 °C for 1 h. The cleavage reaction was initiated by addition of 0.1 mM $Fe(NH_4)_2(SO_4)_2$/0.2 mM EDTA solution, following addition of 0.3% H_2O_2 and 1 mM ascorbic acid. The reaction was allowed to proceed at 42 °C for 2 min and was quenched by the addition of thiourea to a final concentration of 10 mM.

After addition of an equal volume of gel loading buffer (Ambion), the reaction mixture was then separated using 8% polyacrylamide gels containing 7 M urea. The dried gel was imaged by exposure of a phosphor storage plate that was scanned using a PhosphorImager (Molecular Dynamics). The extent of hydroxyl radical protection was quantitated using the ImageQuant software (Molecular Dynamics) as has been described (*13*, *29*). Fractional saturation ($\bar{Y}_i$) of the individual sites was determined from the digitized intensities by nonlinear least-squares fitting of the data against the coupled equations

$$p_i = p_{i,\mathrm{lower}} + (p_{i,\mathrm{upper}} - p_{i,\mathrm{lower}})\bar{Y}_i \quad (1)$$

and

$$\bar{Y}_i = \frac{K_i^{n_\mathrm{H}}[\mathrm{Mg}^{2+}]^{n_\mathrm{H}}}{1 + K_i^{n_\mathrm{H}}[\mathrm{Mg}^{2+}]^{n_\mathrm{H}}} \quad (2)$$

where p_i is the protection of site i, $p_{i,\mathrm{lower}}$ and $p_{i,\mathrm{upper}}$ are the lower and upper transition end points, respectively, K_i is the apparent equilibrium disassociation constant for site i, $[Mg^{2+}]$ is the magnesium concentration, and n_H is the Hill coefficient, which indicates the apparent cooperativity of the transition (*13*, *29*). The data from replicate experiments were individually scaled to $\bar{Y}_i$ and analyzed globally.

Urea-Unfolding Isotherms. The unfolding of RNA folded in the presence of Mg^{2+} was accomplished by urea titration. The solvent accessibility at each point on the isotherms was analyzed by Fe-EDTA footprinting as described above. RNA samples in CE buffer to which was added the indicated concentration of monovalent cation were folded by heating to 95 °C for 1 min and then incubating in the presence of 10 mM $MgCl_2$ at 42 °C. Increasing concentrations of urea were added, and the solutions were incubated at 42 °C for 20 min. The data from replicate experiments were combined and scaled, and each protection was plotted as a function of increasing urea concentration.

Data were analyzed as described previously; briefly, the $\Delta G°_{\mathrm{N-U}}$ and m values were calculated for each unfolding transition curve by direct fitting using the linear extrapolation method (*15*, *30*). This expression is based on fitting a straight line to the baselines before and after the transition region and assuming that $K = F_\mathrm{u}/F_\mathrm{f}$, where K is the equilibrium ratio of unfolded to folded RNA. Use of this equation requires that the unfolding is reversible and that the specific tertiary contacts analyzed are either in a completely folded or unfolded state in the transition region of the isotherm. Two-state folding is typically assumed in analysis of protein unfolding curves derived from fluorescence or CD spectra, in which the curve represents the global unfolding of an entire small protein or domain. Here, the two-state assumption is used for curves that represent a small (one or two base) interaction. Refolding experiments were performed to verify the reaction's reversibility.

RESULTS

Mg^{2+}-Induced Folding of the Isolated P4−P6 Domain. Free radicals generated by a chemical reaction involving the Fe-EDTA complex can cleave solvent-accessible phosphoribose backbone positions. When the RNA folds, sections of the backbone that become inaccessible to solvent are protected from radical cleavage. The extent of protection is correlated with the folding of the molecule (*2*, *13*). The Mg^{2+} dependence of the appearance of protection for eight sites

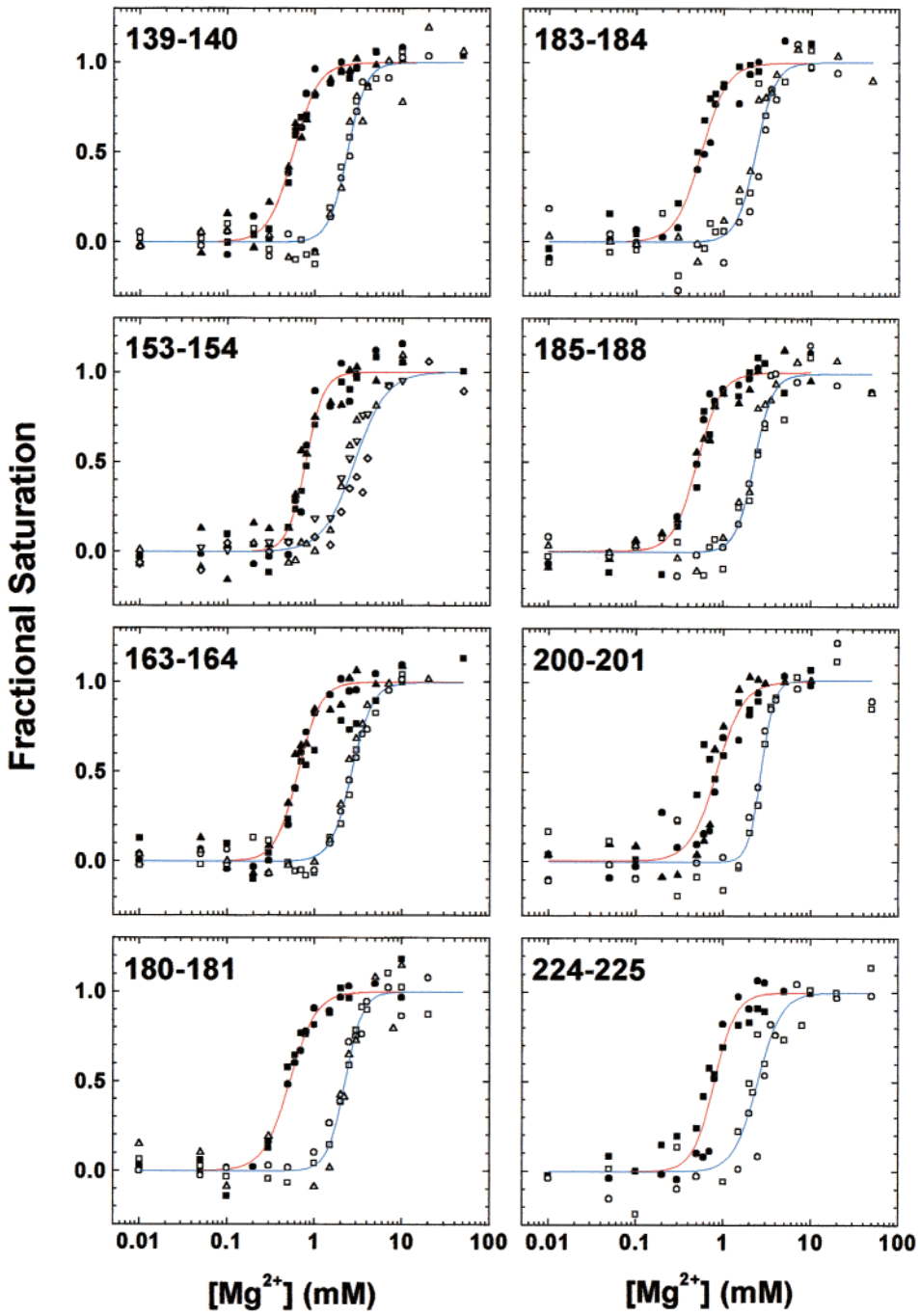

FIGURE 1: Mg^{2+}-folding isotherms of P4−P6 at 10 mM (solid symbols) and 200 mM NaCl (open symbols). The fractional saturation is seen on the *y*-axis. Eight separate protections were monitored, and triplicate experiments were globally fit. The red curve is the fit to the data at 10 mM NaCl, and the blue curve is the fit at 200 mM NaCl.

within P4−P6 was quantitated. Analysis of the data provides two thermodynamic parameters, the equilibrium constant for the transition, K_{Mg}, and the Hill constant, n_H, which reflects the apparent cooperativity of the transition. Eight protections previously examined at 10 mM Na^+ (*13*) were determined at 200 mM Na^+ (Figure 1). Triplicate experiments were globally fit to the equations outlined in the Experimental Procedures section to provide the thermodynamic data shown in Table 1.

At 10 mM NaCl, the K_{Mg} values of the eight discrete protections ranged from 0.5 to 0.8 mM in accordance with those previously reported (*15*, *16*, *24*). The K_{Mg} values for the sites within the A-bulge, including bases 180−181, 183−184, and 185−188, as well as 139−140, which make contacts near the A-bulge, are at the low end of the observed range (0.50−0.56 mM), while the tetraloop and tetraloop-receptor contacts exhibit values near 0.8 mM. Specifically, our results are equal within error to those originally reported by Murphy and Cech at 30 mM Na^+ (*24*), where it was also observed that the protections within the A-bulge (as well as bases 139−140) had midpoints less than those observed elsewhere within P4−P6. The values observed in these two studies are higher than those we have seen in the corresponding regions of the full-length ribozyme (*13*), consistent with the reduced stability of the isolated P4−P6 domain compared to the full-length L-21 (*15*). The Mg^{2+}-folding isotherms obtained at 10 mM Na^+ for the isolated P4−P6 are more cooperative than those for P4−P6 within the full-length ribozyme

Table 1: Equilibrium Data for the Mg-Induced Folding of the Isolated P4−P6 Domain

		[Na$^+$]				[K$^+$]
base		10 mM	50 mM	100 mM	200 mM	200 mM
139−140	K_{Mg}	0.56 ± 0.02	1.2 ± 0.1	1.6 ± 0.1	2.3 ± 0.1	2.0 ± 0.1
	n_H	3.1 ± 0.3	3.0 ± 0.4	4.2 ± 0.5	4.1 ± 0.5	4.5 ± 0.6
153−154	K_{Mg}	0.78 ± 0.03	1.7 ± 0.1	1.8 ± 0.1	2.6 ± 0.2	1.9 ± 0.1
	n_H	4.3 ± 0.7	3.1 ± 0.3	4.4 ± 0.7	2.6 ± 0.4	4.4 ± 0.6
163−164	K_{Mg}	0.65 ± 0.03	1.3 ± 0.1	1.7 ± 0.1	2.6 ± 0.1	1.9 ± 0.1
	n_H	3.4 ± 0.6	3.5 ± 0.5	4.8 ± 0.8	3.7 ± 0.4	5.2 ± 0.5
180−181	K_{Mg}	0.52 ± 0.03	1.0 ± 0.1	1.8 ± 0.1	2.2 ± 0.1	1.8 ± 0.1
	n_H	2.9 ± 0.5	5.2 ± 1.1	4.9 ± 1.4	4.4 ± 0.6	4.1 ± 0.6
183−184	K_{Mg}	0.55 ± 0.03	1.1 ± 0.1	1.6 ± 0.1	2.3 ± 0.1	1.8 ± 0.1
	n_H	2.9 ± 0.5	4.4 ± 1.3	5.5 ± 1.8	4.4 ± 0.8	4.6 ± 0.4
185−188	K_{Mg}	0.50 ± 0.03	1.1 ± 0.1	1.7 ± 0.1	2.2 ± 0.1	2.0 ± 0.1
	n_H	3.2 ± 0.5	3.3 ± 1.2	3.5 ± 0.5	4.1 ± 0.6	4.6 ± 0.5
200−201	K_{Mg}	0.84 ± 0.06	1.3 ± 0.2	1.3 ± 0.1	2.3 ± 0.1	2.0 ± 0.1
	n_H	2.8 ± 0.6	2.9 ± 0.9	3.6 ± 0.8	4.8 ± 1.2	4.1 ± 0.5
224−225	K_{Mg}	0.78 ± 0.04	0.95 ± 0.21	1.4 ± 0.2	2.5 ± 0.3	1.8 ± 0.1
	n_H	4.1 ± 0.9	1.8 ± 0.6	3.0 ± 1.1	2.5 ± 0.7	4.4 ± 0.5

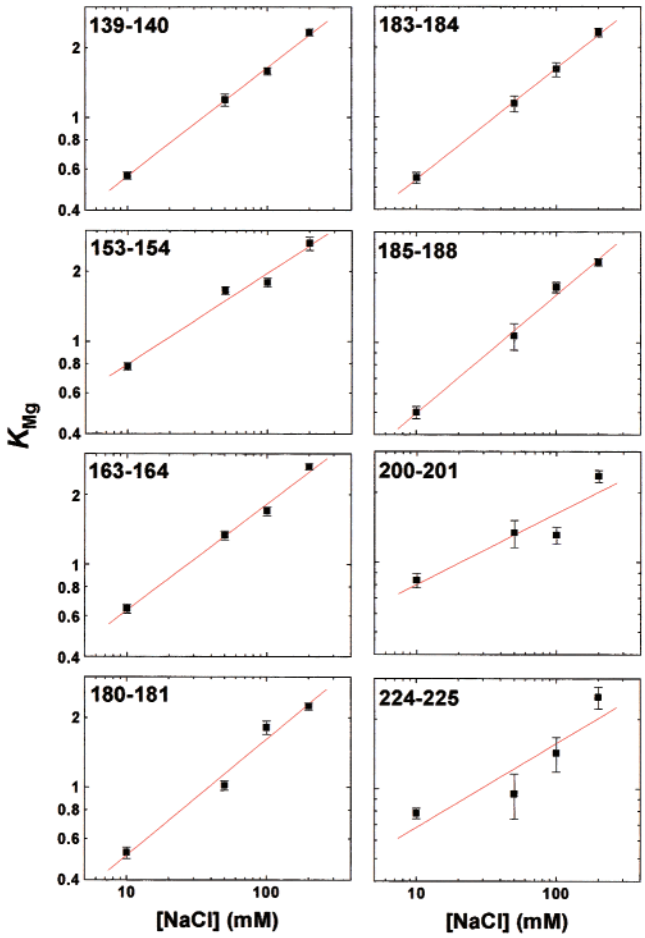

FIGURE 2: $K_{Mg^{2+}}$ is plotted versus [NaCl] with logarithmic scales. The calculated values of δ ln K_{Mg}/δ ln [NaCl] range from 0.3 to 0.5 (see text).

(n_H = 2.8 ± 0.5 to 4.3 ± 0.7, Table 1, vs n_H = 1.9−2.4) (*13*).

[Na$^+$] and [K$^+$] Dependence of Mg^{2+}-Induced Folding. To examine the effect of monovalent ions on P4−P6 folding, Mg^{2+}-folding isotherms for the P4−P6 domain were determined at 10, 50, 100, and 200 mM Na$^+$ and 200 mM K$^+$ (Table 1). The dependence of K_{Mg} on Na$^+$ concentration for all eight sites is summarized in Figure 2. The K_{Mg} values increase as [Na$^+$] is increased. For example, the K_{Mg} value of the protection at nucleotides 185−188 increased about 4-fold (0.50 ± 0.03 to 2.2 ± 0.1 mM) in 200 versus 10 mM Na$^+$ (Table 1). This result demonstrates direct competition between Mg^{2+} and Na$^+$ for the ion binding sites. In addition, the Hill coefficients increased slightly at 200 versus 10 mM Na$^+$, with the average value for all eight sites increasing from 3.3 at 10 mM Na$^+$ to 3.8 at 200 mM Na$^+$. The dependence of Mg^{2+} binding upon NaCl concentration was quantitatively determined from the linkage relationship δ ln K_{Mg}/δ ln [NaCl] (Figure 2) (*31*), yielding clustered values ranging from 0.30 ± 0.08 to 0.51 ± 0.03 for the eight protections of P4−P6. This result indicates a net exchange of less than one ion upon folding.

In the Mg^{2+}-folding experiments conducted at 200 mM KCl, the resolved values of K_{Mg} are smaller than those observed at the same concentration of NaCl (Table 1). The K_{Mg} values in 200 mM K$^+$ are ∼1.9 mM, while the corresponding values at 200 mM Na$^+$ are ∼2.4 mM. The Hill coefficients in K$^+$ are all highly concerted, on the order of ∼4.5 (Table 1). The reduction in K_{Mg} value implies that K$^+$ stabilizes the native form of P4−P6 compared to Na$^+$.

Urea Unfolding at Low and High Salt. Urea denaturation experiments in conjunction with hydroxyl radical footprinting were carried out to further investigate the effect of monovalent ion on stability of the P4−P6 domain. Similar to approaches originally developed to determine the global stability of proteins (*30*), urea unfolding has also been applied to RNA (*32*, *33*). When urea denaturation and footprinting are combined, site-specific unfolding isotherms are generated that can lead to an understanding of both stability changes and cooperative coupling within the molecule (*15*). For a two-state transition with respect to the specific protections examined, a linear dependence of folding free energy on urea concentration is fit to the data to determine the folding free energy at 0 M urea, $\Delta G°_{N-U}$, and the sensitivity to urea denaturation, expressed as the *m* value (*15*, *30*).

Figure 3 shows an autoradiogram of a urea denaturation experiment conducted at 10 mM Mg^{2+} and 200 mM Na$^+$. The Mg^{2+}-folded P4−P6 in the absence of urea is seen in the right-hand lanes (*17*, *18*); clear protections are seen at, for example, base 200 or base 180. As urea is increased in the lanes to the left (*3*−*16*), the protections disappear as the RNA unfolds in the presence of Mg^{2+}. Quantitative analyses of the changes in intensity along a "row" were, as for the Mg^{2+} titrations, carried out for eight hydroxyl radical protections in P4−P6. The results of triplicate experiments at 200 mM Na$^+$ and at 10 mM Na$^+$ were globally analyzed (Figure 4).

Each of the transitions reaches a well-defined end point that is independently established by the Mg^{2+}-free unfolded control lanes (Figure 4, open symbols on the right of each curve). The midpoints of the folding transitions at 200 mM Na$^+$ cluster from 4.0 to 4.7 M (averaging 4.3 M), with *m* values ranging from 0.49 to 0.69 kcal mol^{-1} M^{-1}, yielding $\Delta G°_{N-U}$ values ranging from 2.3 to 2.8 kcal mol^{-1} (Table 2). In contrast, the data for unfolding at 10 mM Na$^+$ have significantly higher midpoints for each protection (Table 2), ranging from 5.4 to 6.9 M (averaging 6.0). This increased stability at low monovalent ion is consistent with the results of the Mg^{2+} titrations (Figure 1).

The protections at nucleotides 180−181, 183−184, and 185−188, which are located in the A-rich bulge, have the

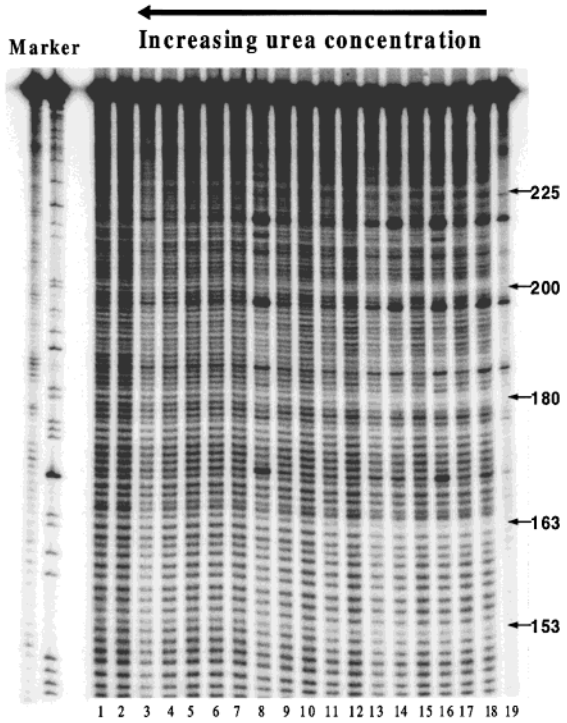

FIGURE 3: Gel image of urea denaturation and Fenton-based footprinting of P4−P6 RNA carried out in 200 mM NaCl and 10 mM Mg^{2+}. Lanes: 1 and 2, unfolded controls (no Mg^{2+}); 3−16, urea concentrations (M) of 7.8, 7.5, 7.0, 6.5, 6.0, 5.5, 5.0, 4.5, 4.0, 3.5, 3.0, 2.5, 2.0, and 1.0; 17 and 18, no urea; 19, no Fenton reagent.

highest $\Delta G°_{N-U}$ values at 10 mM Na^+, 4.5 ± 0.4, 4.2 ± 0.4, and 4.0 ± 0.3 kcal mol^{-1}, respectively, and are consistently higher than the values determined at 200 mM Na^+ (2.3 ± 0.2, 2.6 ± 0.3, and 2.5 ± 0.2 kcal mol^{-1}, respectively). The *m* values range from 0.51 to 0.66 under these conditions. Overall, the average *m* value for the low monovalent ion titration is 0.58 kcal mol^{-1} M^{-1}, comparable to the average of 0.57 observed at 200 mM Na^+. Since the *m* value likely reflects the amount of surface area buried (or exposed) in the folding (unfolding) transition, this result suggests that it is similar for the different conditions (*33*). The largest $\Delta G°_{N-U}$ values are 4.5 kcal mol^{-1} at 10 mM Na^+ and 2.8 kcal mol^{-1} at 200 mM Na^+. These values represent a minimum estimate of the global free energy of unfolding (*15*) and correspond to an increased stability of about 15-fold for P4−P6 at low monovalent ion concentrations.

Urea Unfolding in the Presence of KCl. Urea-unfolding experiments were also carried out in buffer containing 200 mM K^+ rather than Na^+. The midpoints of the isotherms are consistently greater than those for 200 mM Na^+ (averaging 5.2 versus 4.3 M), yielding $\Delta G°_{N-U}$ values larger by 0.3−0.4 kcal mol^{-1} (Table 2). The Mg^+ titration and urea-unfolding results together show 1.5−2-fold greater stability of the P4−P6 RNA in 200 mM KCl compared to the same concentration of NaCl.

DISCUSSION

Monovalent and divalent cations allow nucleic acids to fold into compact, stable structures, overcoming the intrinsic repulsion provided by the charged phosphate anions of the backbone (*34*). RNA stability is dependent on the binding of both delocalized and site-specific cations. Although all cations can function as agents to neutralize negative charge and promote compaction, the role of site-specific cations has been of increasing interest, and the linkage of the effects of monovalent and divalent cations has been a subject of intense study (*9*−*11*, *26*, *31*, *34*−*36*).

Classical studies of transfer RNAs have provided the foundation of our understanding of the thermodynamic and structural basis for metal ion function in the biological activity of RNAs (*37*). Structural studies (*4*, *5*, *38*, *39*) have identified Mg^{2+} ions that are specifically bound to tRNA and have associated these "coordinated" ions with the high-affinity sites (*37*, *40*). However, univalent ions can promote formation of native tRNA structure in the absence of divalent ions (*37*). In addition, some catalytic RNAs can act as catalysts at high concentrations of monovalent ions such as potassium or ammonium, without any divalent ions (*8*, *35*).

Recent thermodynamic analysis of tRNA shows that the crystallographically observed Mg^{2+} binding sites are located in regions of high negative electrostatic potential created by clustering of RNA helices in the formation of tertiary contacts (*36*). Although the ion binding is site-specific, in the sense that a distinct tertiary folding event must occur for the site to form, the Mg^{2+} ions are indicated to retain their hydration shells and thus can fold the RNA while remaining electrostatically bound.

Site-Specific Effects of Monovalent Ions on RNA Folding. The Mg^{2+}-folding and urea-unfolding experiments show that the Mg^{2+}-folded form of P4−P6 is less stable as the monovalent ion concentration is increased. The largest differences in $\Delta G°_{N-U}$ values between 10 and 200 mM Na^+ were observed in the A-bulge at nucleotides 180−181, 183−184, and 185−188 that differ by 2.2, 1.6, and 1.5 kcal mol^{-1}, respectively (Figure 5) compared with differences of 1.0 kcal mol^{-1} for the tetraloop protection and 1.1 kcal mol^{-1} for bases 139−140. The Mg^{2+}-folding isotherms are consistent with these urea-unfolding experiments. Specifically, the midpoints of the folding isotherms for the above protections were lower that those in the rest of P4−P6 at low monovalent ion concentration, while by 200 mM NaCl the midpoints for all eight protections were within the error (Table 1). This implies a more concerted transition in the equilibrium folding mechanism at 200 mM NaCl. However, the differences in midpoints at 10 mM NaCl are not sufficient to support the idea of an equilibrium folding intermediate because the transitions overlap to a significant degree. Instead, one could argue that the distribution of conformations has changed, so that there exists greater homogeneity at higher salt concentrations.

Multiple Mg^{2+} ions coordinated within P4−P6 were evident in the X-ray crystal structure of the isolated domain; these Mg^{2+} ions are shown in green in Figure 5 (*6*). Six of these ions provide a substantial anomalous signal in Mn substitution experiments, and five of these are found in the A-bulge region (*26*). Of the Mg^{2+} ions in the A-bulge, one directly coordinates with nucleotides A184, A186, and A187 and indirectly coordinates with G188. Another Mg^{2+} makes direct inner-sphere coordination to nucleotides A183, A184, and A186. The third Mg^{2+} binds directly to G188 and makes indirect inner-sphere coordination to three nucleotides (C166, U168, and U182). The footprinting data of the A-bulge sites indicate that these Mg^{2+} ions are most affected by changes

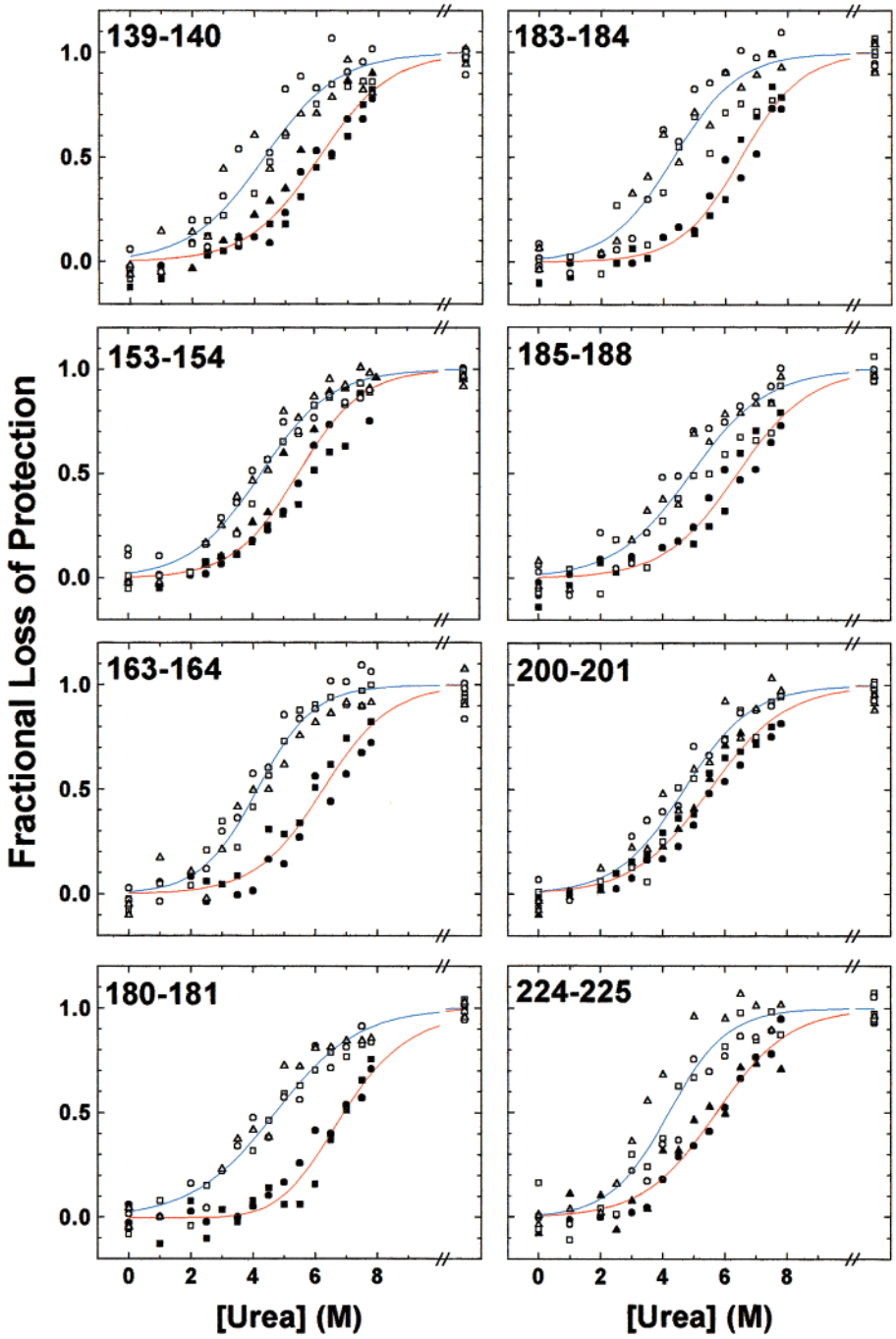

FIGURE 4: Urea-unfolding isotherms at 10 mM (solid symbols) and 200 mM NaCl (open symbols). The scaled extent of protection (1.0 corresponds to unfolded and a loss of protection) is seen on the *y*-axis. Eight separate protections were monitored, and triplicate experiments were globally fit. The red curve is the fit to the data at 10 mM NaCl, and the blue curve is the fit at 200 mM NaCl. The open symbols on the right-hand side of the curves in each graph represent unfolded controls (no Mg^{2+}).

in the monovalent ion concentration. These results are consistent with phosphorothioate substitutions showing that disruption of the Mg^{2+}-site ligation for some of the A-bulge sites destabilizes folding of the P4−P6 domain (*26*).

Comparison of P4−P6 and tRNA. Competition between Na^+ and Mg^{2+} for stabilization of RNA has also been observed for tRNA. However, a 100-fold decrease in K_{Mg} was measured upon increasing the Na^+ concentration from 10 to 170 mM (*40*, *41*). The preference for particular ions in a nucleic acid binding site reflects a complex interplay of forces. In the binding of "delocalized" ions, which play an important role in neutralization of negative charges, the ions are not stripped of their hydration shell (*36*). In contrast, the P4−P6 A-bulge sites involve desolvation of Mg^{2+} ions in the formation of specific contacts with the phosphate oxygens in the sites. The situation in tRNA is, in general, quite different, as the bound Mg^{2+} ions retain their hydration sphere to a greater degree (*36*), providing a reasonable explanation for the difference in thermodynamic linkage between Mg^{2+} and Na^+ ions for tRNA compared to P4−P6. In the former case, Na^+ ions are capable of mediating formation of native structure.

Stabilization of P4−P6 by Potassium. The above arguments are relevant to rationalizing the ability of K^+ to stabilize P4−P6 relative to Na^+ in terms of the specific K^+ binding sites that are observed in the structure of P4−P6

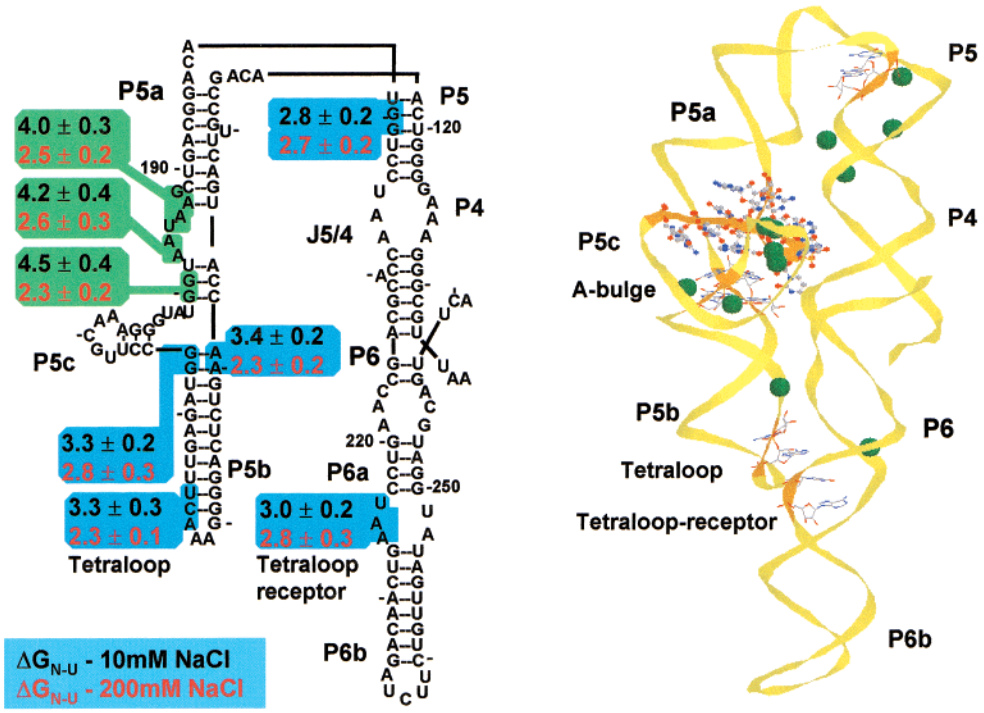

FIGURE 5: The secondary structure of P4−P6 is shown in left-hand panel. The protections examined in this study are colored in blue and green. The three A-bulge protections have a green highlight. ΔG°_{N-U} values for the eight specific protections are shown within the highlights for 10 mM NaCl (black numbers) and 200 mM NaCl (red numbers). The right-hand panel shows a ribbon diagram of P4−P6 based on the crystal structure (*6*). The protection sites are colored orange, and the green spheres are Mg^{2+} ions identified from the crystallographic data.

Table 2: Fitting Results for the Urea-Induced Unfolding of the P4−P6 Domain at Various Salt Concentrations

base	concn (mM)	midpoint (M)	ΔG°_{N-U} (kcal mol^{-1})	*m* (kcal mol^{-1} M^{-1})
139−140	$[Na^+] = 10$	6.2 ± 0.1	3.4 ± 0.2	0.54 ± 0.04
	$[Na^+] = 200$	4.1 ± 0.1	2.3 ± 0.2	0.52 ± 0.05
	$[K^+] = 200$	5.1 ± 0.1	2.7 ± 0.2	0.52 ± 0.03
153−154	$[Na^+] = 10$	5.4 ± 0.2	3.3 ± 0.3	0.60 ± 0.04
	$[Na^+] = 200$	4.1 ± 0.1	2.3 ± 0.1	0.55 ± 0.03
	$[K^+] = 200$	5.2 ± 0.1	2.9 ± 0.2	0.54 ± 0.04
163−164	$[Na^+] = 10$	6.0 ± 0.1	3.3 ± 0.2	0.54 ± 0.04
	$[Na^+] = 200$	4.0 ± 0.1	2.8 ± 0.3	0.69 ± 0.05
	$[K^+] = 200$	5.5 ± 0.1	2.8 ± 0.2	0.51 ± 0.03
180−181	$[Na^+] = 10$	6.9 ± 0.1	4.5 ± 0.4	0.65 ± 0.06
	$[Na^+] = 200$	4.6 ± 0.1	2.3 ± 0.2	0.49 ± 0.03
	$[K^+] = 200$	5.6 ± 0.2	2.8 ± 0.3	0.47 ± 0.06
183−184	$[Na^+] = 10$	6.4 ± 0.1	4.2 ± 0.4	0.64 ± 0.06
	$[Na^+] = 200$	4.2 ± 0.1	2.6 ± 0.3	0.60 ± 0.06
	$[K^+] = 200$	4.9 ± 0.1	2.7 ± 0.3	0.53 ± 0.05
185−188	$[Na^+] = 10$	6.0 ± 0.1	4.0 ± 0.3	0.66 ± 0.04
	$[Na^+] = 200$	4.7 ± 0.1	2.5 ± 0.2	0.51 ± 0.04
	$[K^+] = 200$	5.1 ± 0.1	2.8 ± 0.3	0.53 ± 0.05
200−201	$[Na^+] = 10$	5.4 ± 0.1	2.8 ± 0.2	0.51 ± 0.02
	$[Na^+] = 200$	4.5 ± 0.1	2.7 ± 0.2	0.56 ± 0.04
	$[K^+] = 200$	5.3 ± 0.1	3.1 ± 0.2	0.57 ± 0.04
224−225	$[Na^+] = 10$	5.6 ± 0.1	3.0 ± 0.2	0.53 ± 0.04
	$[Na^+] = 200$	4.0 ± 0.1	2.8 ± 0.3	0.67 ± 0.07
	$[K^+] = 200$	5.2 ± 0.1	3.1 ± 0.4	0.58 ± 0.07

(*9*). Unlike the Mg^{2+} binding sites discussed above, the AA-platform binding sites located within the tetraloop receptor, above the receptor (around base 220), and in the L5c region (Figure 5) have few, if any, phosphate ligands. They consist mostly of polar oxygen and nitrogen ligands. Thus, unfavorable desolvation energetics are much more important in ion binding. The large K^+ ion can shed water molecules more readily than Na^+ while still being satisfied by the weakly coordinating partners. Alternatively, the geometry of the AA-platform binding sites (e.g., the cavity size) is more suited to K^+ ions.

REFERENCES

1. Lindahl, T., Adams, A., and Fresco, J. R. (1966) Renaturation of transfer ribonucleic acids through site binding of magnesium, *Proc. Natl. Acad. Sci. U.S.A. 55*, 941−948.
2. Latham, J. A., and Cech, T. R. (1989) Defining the inside and outside of a catalytic RNA molecule, *Science 245*, 276−282.
3. Gluick, T. C., Gerstner, R. B., and Draper, D. E. (1997) Effects of Mg^{2+}, K^+, and H^+ on an equilibrium between alternative conformations of an RNA pseudoknot, *J. Mol. Biol. 270*, 451−463.
4. Jack, A., Ladner, J. E., Rhodes, D., Brown, R. S., and Klug, A. (1977) A crystallographic study of metal-binding to yeast phenylalanine transfer RNA, *J. Mol. Biol. 111*, 315−328.
5. Quigley, G. J., Teeter, M. M., and Rich, A. (1978) Structural analysis of spermine and magnesium ion binding to yeast phenylalanine transfer RNA, *Proc. Natl. Acad. Sci. U.S.A. 75*, 64−68.
6. Cate, J. H., Gooding, A. R., Podell, E., Zhou, K., Golden, B. L., Kundrot, C. E., Cech, T. R., and Doudna, J. A. (1996) Crystal structure of a group I ribozyme domain: principles of RNA packing, *Science 273*, 1678−1685.
7. Wang, Y. X., Lu, M., and Draper, D. E. (1993) Specific ammonium ion requirement for functional ribosomal RNA tertiary structure, *Biochemistry 32*, 12279−12282.
8. Murray, J. B., Seyhan, A. A., Walter, N. G., Burke, J. M., and Scott, W. G. (1998) The hammerhead, hairpin and VS ribozymes are catalytically proficient in monovalent cations alone, *Chem. Biol. 5*, 587−595.
9. Basu, S., Rambo, R. P., Strauss-Soukup, J., Cate, J. H., Ferre-D'Amare, A. R., Strobel, S. A., and Doudna, J. A. (1998) A specific monovalent metal ion integral to the AA platform of the RNA tetraloop receptor, *Nat. Struct. Biol. 5*, 986−992.
10. Murthy, V. L., and Rose, G. D. (2000) Is counterion delocalization responsible for collapse in RNA folding?, *Biochemistry 39*, 14365−14370.
11. Buchmueller, K. L., Webb, A. E., Richardson, D. A., and Weeks, K. M. (2000) A collapsed non-native RNA folding state, *Nat. Struct. Biol. 7*, 362−366.

12. Russell, R., Millett, I. S., Doniach, S., and Herschlag, D. (2000) Small-angle X-ray scattering reveals a compact intermediate in RNA folding, *Nat. Struct. Biol. 7*, 367−370.
13. Sclavi, B., Woodson, S., Sullivan, M., Chance, M. R., and Brenowitz, M. (1997) Time-resolved synchrotron X-ray "footprinting", a new approach to the study of nucleic acid structure and function: application to protein-DNA interactions and RNA folding, *J. Mol. Biol. 266*, 144−159.
14. Sclavi, B., Sullivan, M., Chance, M. R., Brenowitz, M., and Woodson, S. A. (1998) RNA folding at millisecond intervals by synchrotron hydroxyl radical footprinting, *Science 279*, 1940−1943.
15. Ralston, C. Y., He, Q., Brenowitz, M., and Chance, M. R. (2000) Stability and cooperativity of individual tertiary contacts in RNA revealed through chemical denaturation, *Nat. Struct. Biol. 7*, 371−374.
16. Deras, M. L., Brenowitz, M., Ralston, C. Y., Chance, M. R., and Woodson, S. A. (2000) Folding mechanism of the tetrahymena ribozyme P4−P6 domain, *Biochemistry 39*, 10975−10985.
17. Zarrinkar, P. P., and Williamson, J. R. (1994) Kinetic intermediates in RNA folding, *Science 265*, 918−924.
18. Treiber, D. K., Rook, M. S., Zarrinkar, P. P., and Williamson, J. R. (1998) Kinetic intermediates trapped by native interactions in RNA folding, *Science 279*, 1943−1946.
19. Rook, M. S., Treiber, D. K., and Williamson, J. R. (1998) Fast folding mutants of the *Tetrahymena* group I ribozyme reveal a rugged folding energy landscape, *J. Mol. Biol. 281*, 609−620.
20. Russell, R., and Herschlag, D. (1999) New pathways in folding of the Tetrahymena group I RNA enzyme, *J. Mol. Biol. 291*, 1155−1167.
21. Pan, J., and Woodson, S. A. (1999) The effect of long-range loop-loop interactions on folding of the *Tetrahymena* self-splicing RNA, *J. Mol. Biol. 294*, 955−965.
22. Russell, R., Millett, I., Doniach, S., and Herschlag, D. (2000) Small angle X-ray scattering reveals a compact intermediate in RNA folding, *Nat. Struct. Biol. 7*, 367−370.
23. Pan, J., Deras, M. L., and Woodson, S. A. (2000) Fast folding of a ribozyme by stabilizing core interactions: evidence for multiple folding pathways in RNA, *J. Mol. Biol. 296*, 133−144.
24. Murphy, F. L., and Cech, T. R. (1993) An independently folding domain of RNA tertiary structure within the *Tetrahymena* ribozyme, *Biochemistry 32*, 5291−5300.
25. Silverman, S. K., Deras, M. L., Woodson, S. A., Scaringe, S. A., and Cech, T. R. (2000) Multiple folding pathways for the P4−P6 RNA domain, *Biochemistry 39*, 12465−12475.
26. Cate, J. H., Hanna, R. L., and Doudna, J. A. (1997) A magnesium ion core at the heart of a ribozyme domain, *Nat. Struct. Biol. 4*, 553−558.
27. Zaug, A. J., Grosshans, C. A., and Cech, T. R. (1988) Sequence-specific endoribonuclease activity of the *Tetrahymena* ribozyme: enhanced cleavage of certain oligonucleotide substrates that form mismatched ribozyme-substrate complexes, *Biochemistry 27*, 8924−8931.
28. Celander, D. W., and Cech, T. R. (1991) Visualizing the higher order folding of a catalytic RNA molecule, *Science 251*, 401−407.
29. Brenowitz, M., Senear, D. F., Shea, M. A., and Ackers, G. K. (1986) Quantitative DNase footprint titration: A method for studying protein-DNA interactions, *Methods Enzymol. 130*, 132−181.
30. Santoro, M. M., and Bolen, D. W. (1992) A test of the linear extrapolation of unfolding free energy changes over an extended denaturant concentration range, *Biochemistry 31*, 4901−4907.
31. Record, M. T., Jr., Anderson, C. F., and Lohman, T. M. (1978) Thermodynamic analysis of ion effects on the binding and conformational equilibria of proteins and nucleic acids: the roles of ion association or release, screening, and ion effects on water activity, *Q. Rev. Biophys. 11*, 103−178.
32. Shelton, V. M., Sosnick, T. R., and Pan, T. (1999) Applicability of urea in the thermodynamic analysis of secondary and tertiary RNA folding, *Biochemistry 38*, 16831−16839.
33. Fang, X., Pan, T., and Sosnick, T. R. (1999) A thermodynamic framework and cooperativity in the tertiary folding of a Mg^{2+}-dependent ribozyme, *Biochemistry 38*, 16840−16846.
34. Shiman, R., and Draper, D. (2000) Stabilization of RNA Tertiary Structure by Monovalent Cations, *J. Mol. Biol. 302*, 79−91.
35. Pyle, A. M. (1996) Role of metal ions in ribozymes, *Met. Ions Biol. Syst. 32*, 479−520.
36. Misra, V., and Draper, D. (2000) Mg^{2+} Binding to tRNA Revisited: The Non-Linear Poisson Boltzman Model, *J. Mol. Biol. 299*, 813−815.
37. Schimmel, P. R., and Redfield, A. G. (1980) Transfer RNA in solution: selected topics, *Annu. Rev. Biophys. Bioeng. 9*, 181−221.
38. Hingerty, B., Brown, R., and Jack, A. (1978) Further refinement of the structure of yeast $tRNA^{Phe}$, *J. Mol. Biol. 124*, 523−534.
39. Westhof, E., and Sundaralingam, M. (1986) Restrained refinement of the monoclinic form of yeast phenylalanine transfer RNA, *Biochemistry 25*, 4868−4878.
40. Rialdi, G., Levy, J., and Biltonen, R. (1972) Thermodynamic studies of transfer ribonucleic acids. I. Magnesium binding to yeast phenylalanine transfer ribonucleic acid, *Biochemistry 11*, 2472−2479.
41. Stein, A., and Crothers, D. M. (1976) Equilibrium binding of magnesium (II) by Escherichia coli tRNAfMet, *Biochemistry 15*, 157−160.

BI020042V